Theoretical Chemistry Accounts (2022) 141:38
https://doi.org/10.1007/s00214-022-02896-4

REGULAR ARTICLE

A DFT theoretical investigation on the interplay effects between cation-π and intramolecular hydrogen bond interactions in the mesalazine···Fe^{2+} binary complex

Marziyeh Mohammadi[1] · Fatemeh Hoseinpour[1] · Azadeh Khanmohammadi[2]

Received: 1 February 2022 / Accepted: 19 June 2022 / Published online: 13 July 2022

Abstract
A detailed study on mesalazine···Fe^{2+} complex is performed using density functional theory calculations to show the interplay effects of cation–π and intramolecular hydrogen bond (IMHB) interactions in the presence of the different solvents. To achieve better insight on the mentioned interactions, the complex of benzene and the mesalazine analogue is chosen as a set of reference points. For this purpose, the analyses of atoms in molecules and natural bond orbital are applied to study the nature of the bonding. The results exhibit that the coexistence of IMHB and cation–π interactions decreases the IMHB strength and increases the cation–π interactions. The electronic properties, stability and reactivity of the studied complex in the various solvents are also evaluated by frontier molecular orbitals, chemical hardness as well as electronic chemical potential.

Keywords Cation–π · Intramolecular hydrogen bond · DFT · AIM · NBO

1 Introduction

Mesalazine (5-aminosalicylic acid or mesalamine), the active moiety of sulfasalazine (salazosulfapyridine), is available for the treatment of active ulcerative colitis of mild-to-moderate severity [1, 2]. It is an organic compound with the chemical formula $C_7H_7NO_3$. Ulcerative colitis causes inflammation of the intestine which leads to problems such as ulceration and bleeding. Crohn's disease is also a condition which causes inflammation of any part of the gastrointestinal system. Aminosalicylates are a group of medicines commonly used to treat inflammatory bowel diseases [3]. Mesalazine (MES) is one of the most commonly used aminosalicylates. Although it is not clear exactly how MES works, it is thought to act on cells lining the intestine to change the way these cells make and release certain chemicals. It allows the damaged intestine to recover and helps to prevent symptoms from flaring up again.

✉ Marziyeh Mohammadi
m.mohammadi@vru.ac.ir

[1] Department of Chemistry, Faculty of Science, Vali-e-Asr University of Rafsanjan, P. O. Box: 77176, Rafsanjan, Iran

[2] Department of Chemistry, Payame Noor University, PO Box 19395-3697, Tehran, Iran

Noncovalent interactions (NCIs) such as hydrogen bond, cation–π, anion–π and π–π are important in the field of biomolecular structure and function [4–10]. The hydrogen bond (HB), in particular, is one of the most important interactions present in different biological activities [11–13]. In supramolecular chemistry, it has been believed that the HB is able to control and direct the structures of molecular assemblies because it is sufficiently strong and directional [13–18]. Cation–π interactions, as another ensemble of NCIs, are of prime importance in several areas of contemporary interest, such as chemistry, material science, biology, and allied areas [19–23]. This interaction is essentially electrostatic in origin because a positively charged cation interacts with negatively charged electron cloud of π-systems [24–26]. The induction (induced polarization) interactions are also the major source of the attraction in the cation–π interaction [27], and the contribution of the dispersion interaction is relatively small in these interactions.

The interplay between NCIs is effective for understanding some biological processes [28, 29]. Numerous theoretical studies have been devoted to the elucidation of the interplay between cation–π and HB interactions. For instance, Li et al. [30] evaluated the role of methyl group in the cooperativity between cation–π and NH···O hydrogen bond interactions. In 2020, the enhancing effect of the cation–π interaction on the intramolecular HB in acetaminophen complex investigated

by Mohammadi et al. [31]. Mutual effects of the cation–π, anion–π and intramolecular HB in the various complexes of 1,3,5-triamino-2,4,6-trinitrobenzene with some cations (Li^+, Na^+, K^+, Mg^{2+}, Ca^{2+}) and anions (F^-, Cl^-, Br^-) explored by Nowroozi et al. [32]. Also, Alirezapour et al. [33] analyzed the cation–π interactions effect on the strength and nature of the intramolecular HB in the various complexes of para aminosalicylic acid with Cr^{2+}, Mn^+, Fe^{2+}, Co^+, Ni^{2+}, Cu^+ and $Zn.^{2+}$ cations. Finally, the interplay among three important NCIs involving aromatic rings such as HB, cation–π and π–π interactions studied using ab initio calculations by Estarellas et al. [34].

Metal ions are essential elements for healthy life to humans [35]. For instance, the transition-metal ions participate in biological systems as multiplied charged ions, which bind more strongly to ligands due to increased electrostatic potential and smaller ionic radius with respect to non-transition-metal ions [36]. The current paper depicts a comprehensive study on interaction of the MES drug with Fe^{2+} cation in the presence of several different solvents. Our objective from this work is to explore the interplay effects of IMHB and cation–π interactions on the geometrical parameters, spectroscopic data, binding energies and topological properties. For this purpose, the DFT calculations along with the AIM and NBO analyses are exploited. Finally, we have performed an inclusive analysis of molecular orbital energies to evaluate the electronic properties, stability and reactivity of the analyzed complex.

2 Computational methods

All theoretical calculations are performed with the Gaussian 03 software package [37] using the wB97XD method and the 6-311++G(d,p) basis set. This method has been proved to be reliable for the study of noncovalent complexes [38–42]. The calculations are carried out in the presence of several different solvents (water, ethanol, acetone, chloroform, ether and carbon tetrachloride) using the self-consistent reaction field (SCRF) method with the polarized continuum model (PCM) [43]. Vibrational frequencies are estimated at the same level to verify that all the stationary points correspond to the true minima on the potential energy surface as well as to obtain the zero-point vibrational energies (ZPVE) that contribute to the total energy.

The binding energy, ΔE, can be evaluated from the difference between energy of the complex and sum of the energies of cation and π-system as given in Eq. (1):

$$\Delta E = E_{\text{cation}-\pi} - \left(E_{\text{cation}} + E_{\pi-\text{system}}\right) + E_{\text{BSSE}} \quad (1)$$

Based on this formula, $E_{\text{cation}-\pi}$ is the total energy of complex and E_{cation} and $E_{\pi\text{-system}}$ are referred to the total energies of isolated cation and MES (or BEN) monomer, respectively. The E_{BSSE} is the basis set superposition error (BSSE) corrected for the binding energies [44]. The obtained wave functions are used for the topological analysis of the electron density by using the AIM method [45]. These calculations are performed with the AIM 2000 program package [46]. The NBO analysis [47] is employed to evaluate the charge transfer process during the complex formation. Finally, the DFT-based global reactivity indices such as energy gap, softness (S), chemical hardness (η) [48], electronic chemical potential (μ) [49], electrophilicity index (ω) [50] and electronegativity (χ) [51] are considered with the calculation of the highest occupied molecular orbital (HOMO) and the lowest unoccupied molecular orbital (LUMO) energies by the following equations:

$$\eta = \frac{\left(E_{\text{LUMO}} - E_{\text{HOMO}}\right)}{2} \quad (2)$$

$$\mu = \frac{\left(E_{\text{LUMO}} + E_{\text{HOMO}}\right)}{2} \quad (3)$$

$$\omega = \frac{\mu^2}{2\eta} \quad (4)$$

$$S = \frac{1}{2\eta} \quad (5)$$

3 Results and discussions

In the present research, an implicit-solvent model has been considered in the presence of different solvents for the MES···Fe^{2+} complex. Implicit (continuum) solvation is a method to represent solvent as a continuous medium (solvent molecules are replaced by a homogeneously polarizable medium) instead of individual "explicit" solvent molecule. The main parameter used to indicate the solvent is the dielectric constant (ε). Explicit models consider molecular details of each solvent molecule.

3.1 Energetic descriptors

In this section, we intend to investigate the interplay effects between cation–π and IMHB interactions on the mesalazine complex (MES···Fe^{2+}) as a benchmark system in the different solvents. To gain a detailed insight, the parent molecule (MES) and the benzene complex (BEN···Fe^{2+}) are chosen as a set of reference points. The obtained structures for these complexes are shown in Fig. 1. As given in Table 1, the

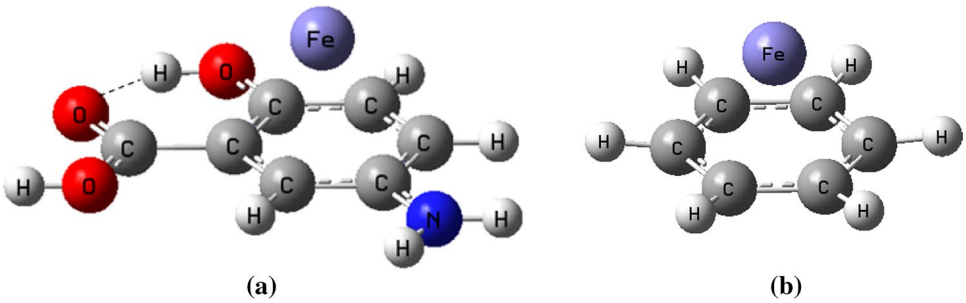

Fig. 1 Molecular structure of **a** MES···Fe^{2+} and **b** BEN···$Fe.^{2+}$ complexes at the wB97XD/6-311++G(d,p) level of theory

Table 1 BSSE-corrected binding and IMHB energies (ΔE_{BSSE} and E_{HB}, in kcal mol^{-1}), the geometrical (bond lengths (d), in Å and bond angles (θ), in °), spectroscopic descriptors (ν, in $cm.^{-1}$) and charge density on metal cation (q_{ion}, in e) of complexes calculated at the wB97XD/6-311++G(d,p) level of theory

	ΔE_{BSSE}	$d_{ion\ldots\pi}$	$\nu_{ion\ldots\pi}$	q_{ion}	E_{HB}	d_{O-H}	$d_{H\ldots O}$	θ_{OHO}	ν_{O-H}
BEN···Fe^{2+}					*MES*				
Water	−19.50	1.564	356.9	0.908	−11.94	0.975	1.769	144.8	3582.2
Ethanol	−23.52	1.566	357.8	0.886	−11.90	0.975	1.770	144.9	3586.4
Acetone	−24.72	1.566	349.4	0.884	−11.89	0.975	1.770	144.9	3587.3
Chloroform	−49.83	1.568	365.7	0.795	−11.74	0.975	1.774	144.7	3597.6
Ether	−53.87	1.567	349.4	0.790	−11.71	0.975	1.775	144.6	3598.7
CCl_4	−90.38	1.570	354.2	0.706	−11.56	0.974	1.779	144.4	3607.1
MES···Fe^{2+}					*MES···Fe^{2+}*				
Water	−22.28 (8.41)	1.598	417.6	0.865	−11.63	0.981	1.770	143.0	3500.6
Ethanol	−26.85 (5.35)	1.597	419.0	0.845	−11.60	0.981	1.771	142.9	3497.1
Acetone	−28.41 (4.31)	1.595	419.2	0.841	−11.52	0.981	1.773	142.8	3502.4
Chloroform	−58.07 (−17.22)	1.598	418.6	0.738	−11.58	0.983	1.772	141.9	3476.7
Ether	−62.31 (−21.02)	1.598	420.6	0.731	−11.57	0.983	1.772	141.9	3475.0
CCl_4	−104.20 (−58.28)	1.600	423.6	0.640	−11.46	0.984	1.775	140.8	3458.5

*Values in parentheses refer to the obtained binding energies in the high-spin state (quintet for the MES···Fe^{2+} complex in different solvents)

interaction strength of the MES···Fe^{2+} and BEN···Fe^{2+} complexes in different solvents is as follows:

water < ethanol < acetone < chloroform < ether < CCl_4

It is clear that the strongest/weakest interactions belong to the CCl_4/water solvents, respectively. Hence, formation of these complexes in the non-polar solvents is more favorable with respect to the polar ones.

In this study, Fe^{2+} is an open-shell system, with a d^6 configuration, and there are three different spin states (singlet, triplet and quintet). The low-spin (LS) state is the singlet and the high-spin (HS) state the quintet. Because the spin multiplicity of the MES···Fe^{2+} complex is considered the singlet, hence, it is the low spin. In order to confirm the stability, we have also been performed the high-spin state (quintet) for the selected complex in the different solvents. As shown in Table 1, the low-spin state of the complex is more stable than its high-spin state.

The results of binding energy show that the presence of HB increases the strength of cation–π interaction. The transfer of electron density from the quasi-ring created by the formation of HB to the benzene ring probably increases the strength of the cation–π interaction in the MES complex. The charge density on metal cations (q_{ion}) is another factor that affects these interactions (see Table 1). As shown in this table, these values for MES complex are smaller than BEN one. This means that the charge transfer from the bonding orbitals of the C–C bond of benzene ring to LP^*_{cation} (antibond lone pair) for MES complex is higher than BEN complex.

In the current research, the HB energy (E_{HB}) could be estimated from the properties of bond critical points. The simple relationship between the E_{HB} and the potential energy density $V(r_{cp})$ at the critical point corresponding to H···O contact is assigned to be $E_{HB} = 1/2\ V(r_{cp})$ [52–54]. Our findings reveal that the E_{HB} of the MES complex in the different media is lower than the parent molecule (see Table 1). This means that the coupling of IMHB and cation–π interactions

reduces the strength of HB. It can probably be due to the attraction effect between the Fe^{2+} cation and π-electrons of the benzene ring that diminishes the electron density within the quasi-ring of HB and leads to the reduction of the E_{HB}. However, the order of the decreased HB energies of MES complex with respect to its corresponding monomer is as chloroform (0.16) > ether (0.14) > CCl_4 (0.10 kcal mol^{-1}) for the non-polar solvents and acetone (0.37) > water (0.31) > ethanol (0.30 kcal mol^{-1}) for the polar ones.

3.2 Geometric descriptors

In this section, in order to study the strength of the cation–π interactions, the distance among the ion and the middle of the aromatic ring ($d_{ion\cdots_\pi}$) for the studied complexes is calculated. The $d_{ion\cdots_\pi}$ is one of structural parameters that can influence the strength of the cation–π interactions. A comparison of the strength of these interactions and $d_{ion\cdots_\pi}$ shows a reverse relationship between them. Based on our theoretical results, with the exception of MES complex in the polar solvents, a meaningful relationship cannot be observed between the computed $d_{ion\cdots_\pi}$ values and the achieved binding energies in the other complexes (see Table 1). As shown in this table, the obtained values of $d_{ion\cdots_\pi}$ for MES complex are greater than the corresponding values of BEN complex, which means that the presence of IMHB does not confirm the strengthening of the cation–π interaction of the MES complex in these solvents.

For investigating of the cation–π interaction influence on the strength of IMHB, the geometrical parameters of the quasi-ring created by the formation of HB are analyzed. It is prominent that the HB distances and the corresponding angles are important characteristics that can influence HB strength [55]. For a strong HB system, the elongation of the O–H bond length as proton donor, the shortening of the H···O distance as proton acceptor and the increment of the O–H···O angle are accompanied with an increase in the HB strength. However, the O–H···O interaction should be virtually designated as O···H···O (or O–H–O) since for the energetic minimum the proton is placed in the middle of O···O distance or nearly so [56, 57] and both the H···O interactions are equivalent. The calculated structural parameters for MES complex in the different solvents are collected in Table 1.

As observed in this table, in comparison with the geometrical parameters obtained for the MES complex, the parent molecule (MES), in most cases, has the smallest the $d_{O\text{-}H}$ and $d_{H\cdots O}$ and the greatest the θ_{OHO}. On the other hand, the results show that the coupling of cation–π and IMHB interactions increases the $d_{O\text{–}H}$ and $d_{H\cdots O}$ (except for non-polar solvents) and also, decreases the θ_{OHO} values at the HB critical points of the MES complex. This means that the presence of cation–π interaction diminishes the IMHB strength. There is good linear relationship between the E_{HB} and $d_{H\cdots O}$ values with correlation coefficient (R^2) equal to 0.9801 (see Fig. 2). In contrast, the corresponding correlation cannot be found for the E_{HB} and $d_{O\text{–}H}$. In other words, the $d_{H\cdots O}$ correlates better with the E_{HB} with respect to the $d_{O\text{–}H}$. However, as shown in Fig. 3, the $d_{O\text{–}H}$ results correlate very well with the binding energies.

3.3 Spectroscopic descriptors

Shifting of stretching frequencies is also applied to investigate the mutual effects between the cation–π and IMHB interactions. The ion···π stretching frequencies ($\nu_{ion\cdots_\pi}$) computed for all of complexes in the presence of different solvents are reported in Table 1. It is well-established that the stronger the cation–π interaction is accompanied with the larger

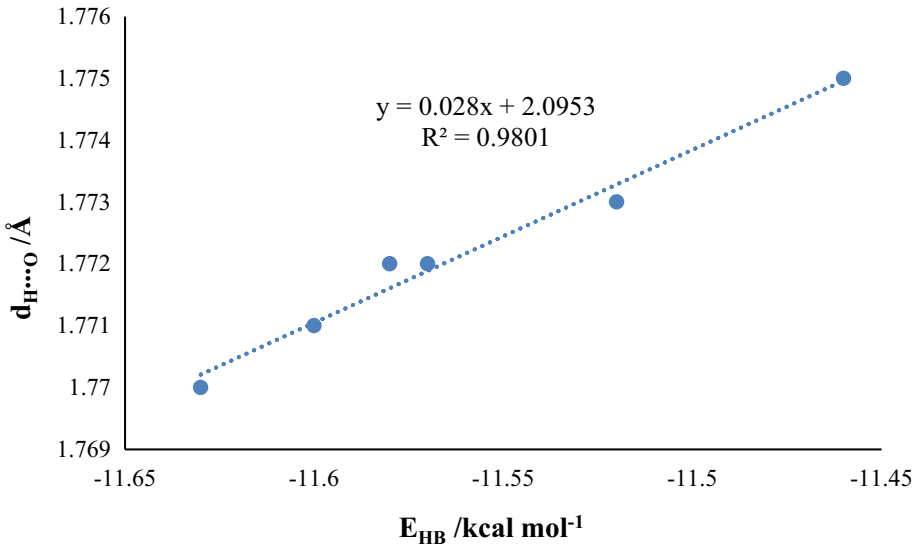

Fig. 2 Correlation between the $d_{H\cdots O}$ and the E_{HB} values

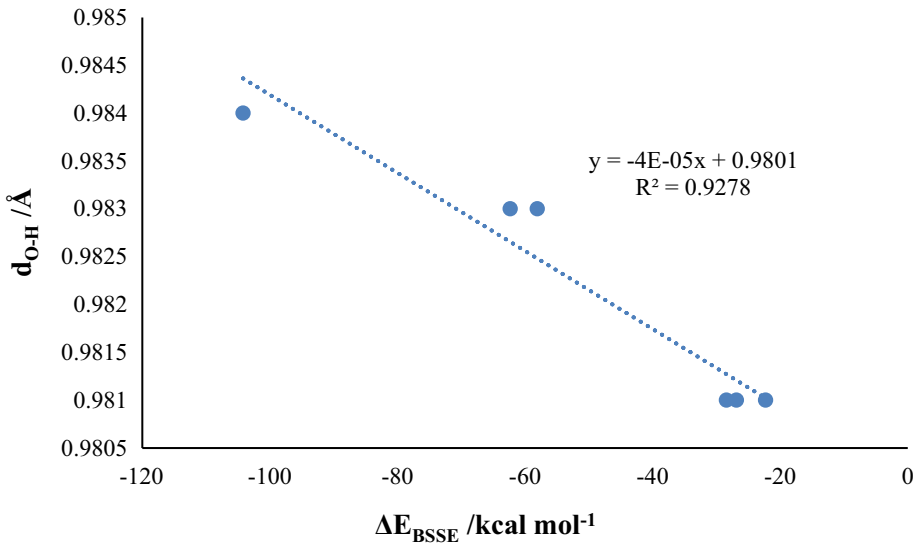

Fig. 3 Relation between the d_{O-H} and ΔE_{BSSE} values

the shifting. The theoretical results show that the values of $\nu_{ion\cdots\pi}$ for the MES and BEN complexes are in the ranges of 418–424 cm^{-1} and 349–366 cm^{-1}, respectively. Our data display a meaningful relationship between the calculated $\nu_{ion\cdots\pi}$ values and the obtained binding energies (see Table 1). As revealed in this Table, the increased $\nu_{ion\cdots\pi}$ value for MES complex in the acetone solvent with respect to the corresponding value of BEN complex is about 70 cm^{-1}; as a result, the coexistence of the IMHB and cation–π interactions strengthens the cation–π interaction of the selected complex in these solvents.

The frequency stretching mode (ν_{O-H}) of corresponding to the O–H···O HB is also investigated to achieve better insight on the nature of the IMHB in the presence of the cation–π interactions (see Table 1). One can see the typical for conventional HBs red shift of the stretching mode. The lengthening of the proton-donating bond as an effect of HB formation is accompanied with the redshift of the corresponding mode. The results of Table 1 show that in the presence of cation–π interactions, the values of ν_{O-H} decrease. Therefore, with the coupling of cation–π and IMHB interactions, the HB strength of MES complex diminishes with respect to the parent molecule. The results display that the O–H stretching frequencies (ν_{O-H}) for the MES complex relative to those of its monomer in the different solvents show red-shifted by ca. CCl_4 (149) > ether (124) > chloroform (121) > ethanol (89) > acetone (85) > water (82 cm^{-1}), which are well-correlated with the O–H bond lengths (d_{O-H}) upon HB formation (see Table 1). Therefore, the $\Delta\nu_{O-H}$ can be easily evaluated from the d_{O-H}, as follows:

$$\Delta\nu_{O-H} = 20132d_{O-H} - 19665, \quad R^2 = 0.9832$$

It is also interesting to note that the binding energies (ΔE_{BSSE}) have excellent linear correlation with the values of ν_{O-H} (see Fig. 4).

To confirm the correlations presented in Figs. 2, 3, and 4, we have changed the distance between Fe^{2+} and benzene ring from 1.0 to 4.0 Å with the step size of 0.1 Å. The flexible scans are performed for the MES complex in ether (non-polar) and water (polar) solvents. The correlations with Figs. S1 to S6 are shown in the Supplementary section. The obtained results indicate that Figs. 2, 3, and 4on the specified distances are satisfactory. While calculating the scan, the COOH functional group attached to the benzene ring comes out of the flat position. This causes the OH oxygen of the COOH group to interact with the Fe^{2+} cation. Perhaps this is why these correlations are established in certain distances.

3.4 Topological descriptors

The AIM theory [45, 58] gives depictions of different kinds of the bonding and atomic interactions according to the ideas of descriptive chemistry. It is based on the analysis of the bond critical point (BCP) of electron density (ρ), its Laplacian ($^2\rho$) and the other properties such as the local kinetic electron energy density (G), the local potential electron energy density (V) and the total electron energy density (H). Figure 5 demonstrates the molecular graphs of the studied complexes in this manuscript. As shown in this figure, the bond paths are formed between the metal ion and the carbon atoms of aromatic ring.

It is well-known that the electron density properties at the BCPs of cation–π, $\rho(r)_{ion\cdots\pi}$, may be a valuable factor for depicting the strength of ion–π interactions [59]. The results of AIM analysis are summarized in Table 2. As observed in this table, the coupling of the quasi-ring of HB and benzene ring increases the $\rho(r)_{ion\cdots\pi}$ values for the MES···Fe^{2+} complex with respect to the BEN···Fe^{2+} one. It is clear from Table 2 that the increased $\rho(r)_{ion\cdots\pi}$

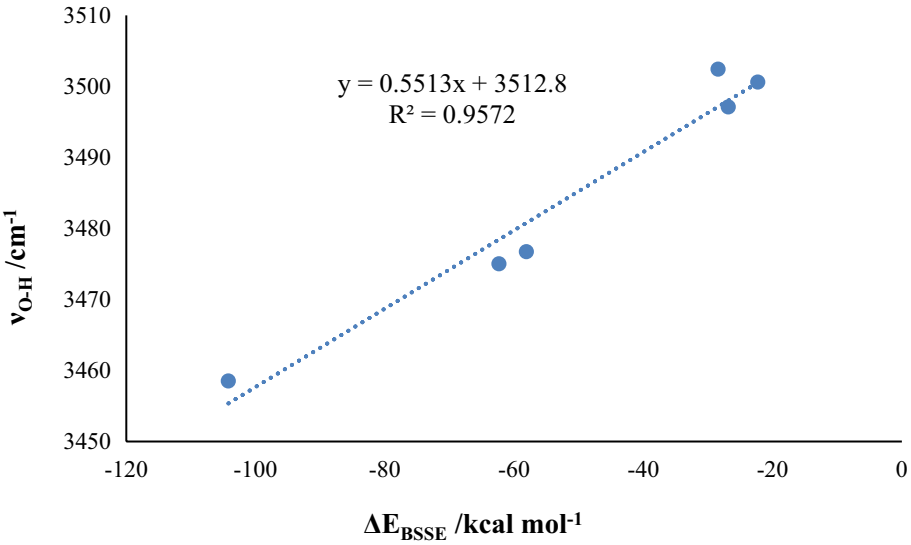

Fig. 4 Relation between the ν_{O-H} and ΔE_{BSSE} values

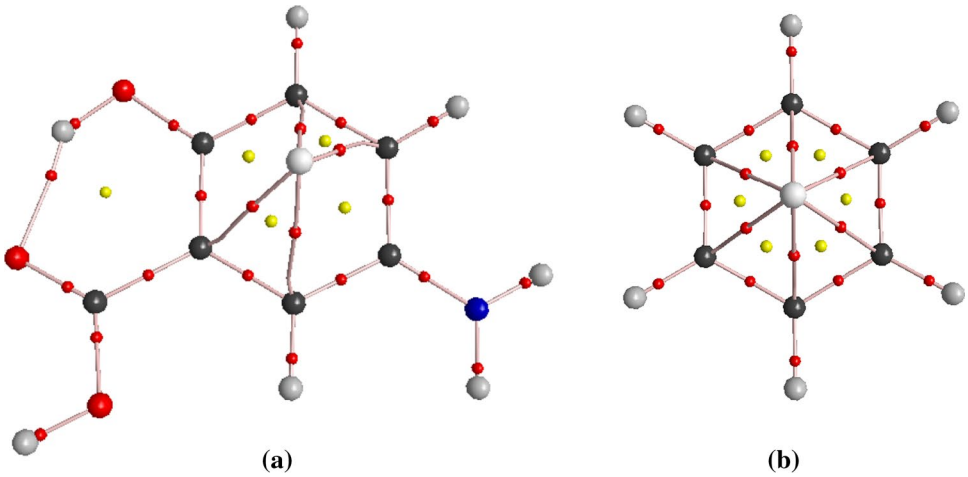

Fig. 5 Typical molecular graphs obtained from AIM analysis for **a** MES···Fe^{2+} and **b** BEN···$Fe.^{2+}$ complexes. The small red, yellow spheres, and lines correspond to bond critical points (BCPs), ring critical points (RCPs) and bond paths, respectively

Table 2 Selected topological properties of electron density (in a.u.) obtained by AIM analysis

	ion···π					HB				
	ρ(r)	$\nabla^2\rho$(r)	H(r)	V(r)	–G/V	ρ(r)	$\nabla^2\rho$(r)	H(r)	V(r)	–G/V
BEN···Fe^{2+}						*MES*				
Water	0.0816	0.2278	−0.0251	−0.1072	0.766	0.0401	0.1331	−0.0024	−0.0380	0.938
Ethanol	0.0814	0.2282	−0.0249	−0.1068	0.767	0.0399	0.1328	−0.0023	−0.0379	0.938
Acetone	0.0813	0.2276	−0.0248	−0.1066	0.767	0.0399	0.1328	−0.0023	−0.0379	0.938
Chloroform	0.0812	0.2265	−0.0249	−0.1064	0.766	0.0396	0.1319	−0.0022	−0.0374	0.941
Ether	0.0811	0.2261	−0.0247	−0.1060	0.767	0.0395	0.1317	−0.0022	−0.0373	0.942
CCl_4	0.0806	0.2248	−0.0244	−0.1051	0.767	0.0391	0.1308	−0.0021	−0.0368	0.944
MES···Fe^{2+}						*MES···Fe^{2+}*				
Water	0.0852	0.2537	−0.0262	−0.1158	0.774	0.0397	0.1255	−0.0028	−0.0370	0.924
Ethanol	0.0863	0.2353	−0.0288	−0.1164	0.753	0.0397	0.1253	−0.0028	−0.0369	0.924
Acetone	0.0865	0.2359	−0.0289	−0.1168	0.752	0.0395	0.1250	−0.0027	−0.0367	0.926
Chloroform	0.0867	0.2348	−0.0292	−0.117	0.751	0.0396	0.1252	−0.0028	−0.0369	0.925
Ether	0.0868	0.2354	−0.0293	−0.1174	0.751	0.0396	0.1252	−0.0028	−0.0368	0.925
CCl_4	0.0873	0.2346	−0.0298	−0.1183	0.748	0.0393	0.1247	−0.0027	−0.0365	0.927

values for the MES complex in comparison with the corresponding values of the BEN complex are as: CCl_4 (0.0067) > ether (0.0057) > chloroform (0.0055) > acetone (0.0052) > ethanol (0.0049) > water (0.0036 a.u.). As can be seen, these changes for the MES···Fe^{2+} complex in the non-polar solvents are higher than the polar ones. There is a good relatively linear relationship between the $\rho(r)_{ion\cdots\pi}$ values and the binding energies ($R = 0.8068$), which means that the effect of the HB on the $\rho(r)_{ion\cdots\pi}$ values may be dependent on the type of the solvent.

The electron density at the BCP of HB ($\rho(r)_{H\cdots O}$) can also be considered as one of the indicators of HB strength. As can be seen in Table 2, the trend in ($\rho(r)_{H\cdots O}$) charge densities is as follows: water (0.0397) ≈ ethanol (0.0397) > acetone (0.0395 a.u.) for the polar solvents and ether (0.0396) ≈ chloroform (0.0396) > CCl_4 (0.0393 a.u.) for the non-polar ones. This arrangement is almost identical to the obtained parameters of E_{HB}. In addition, the greatest $\rho(r)_{H\cdots O}$ values are observed in the parent molecule with respect to those found in the MES complex (except for ether and CCl_4 solvents), which indicates the presence of cation–π interaction decreases the IMHB strength. Another parameter that can affect the nature of NCIs is the −G/V ratio [60, 61]: for $-G/V \geq 1$, the interaction is electrostatic, while for $0.5 < -G/V < 1$, it is partly covalent. As observed in Table 2, the computed $-G/V_{ion\cdots\pi}$ and $-G/V_{H\cdots O}$ values prove that the analyzed complexes are partly covalent.

3.5 Charge transfer descriptors

The NBO analysis explains the most important orbital interactions in order to clarify general structural features [62]. The results of NBO analysis show that the donor–acceptor interaction energies, $E^{(2)}$, reported in Table 3 are related to the dominant interaction of $\sigma_{(C-C)} \rightarrow LP^*_{(cation)}$, which is between the σ-electrons of donor species and the LP* of cation as acceptor agent. As shown in this table, the coexistence of the IMHB and cation–π interactions increases the donor–acceptor interaction energies, $E^{(2)}$, of the MES···Fe^{2+} complex. This result can be contributed to the strengthening of cation–π interaction in this complex with respect to the BEN one. For instance, the $E^{(2)}$ value for the MES···Fe^{2+} complex in the water solvent is higher than the corresponding value of the BEN···Fe^{2+} (about 0.65 kcal mol^{-1}).

The value of charge transfer ($\Delta q_{(CT1)}$) between the aromatic ring and a cation is easily estimated as the difference between the atomic charge of the free cation and the complexed cation. The theoretical results indicate that the simultaneous presence of cation–π and IMHB interactions enhances the values of $\Delta q_{(CT1)}$ for the MES complex with respect to the BEN one (see Table 3), which are directly proportional to the obtained $E^{(2)}$ values. Hence, the charge transfer may be a helpful characteristic for evaluating the strength of these interactions.

In the NBO analysis of HB systems, the charge transfer between the lone pairs of proton acceptor and the anti-bonds

Table 3 Values of $E^{(2)}$ correspond to $\sigma_{(C-C)} \rightarrow LP^*_{(cation)}$ and $LP_{(O)} \rightarrow \sigma^*_{(O-H)}$ interactions (in kcal $mol.^{-1}$), occupation numbers of donor (ON_D) and acceptor (ON_A) orbitals, charge density on oxygen atom (q_O, in e) and the charge transfers ($\Delta q_{(CT)}$, in e) of the studied complexes in the presence of different solvents

	ion···π interaction				HB interaction				
	$\sigma_{(C-C)} \rightarrow LP^*_{(cation)}$				$LP_{(O)} \rightarrow \sigma^*_{(O-H)}$				
	$E^{(2)}$	$ON_{\sigma(C-C)}$	$ON_{LP^*_{(cation)}}$	$\Delta q_{(CT1)}$	$E^{(2)}$	$ON_{LP(O)}$	$ON_{\sigma^*(O-H)}$	q_O	$\Delta q_{(CT2)}$
BEN···Fe^{2+}					*MES*				
Water	4.35	0.9773	0.0516	1.092	15.31	1.8551	0.0383	−0.385	–
Ethanol	4.33	0.9775	0.0516	1.114	15.27	1.8550	0.0382	−0.384	–
Acetone	4.32	0.9775	0.0515	1.116	15.27	1.8550	0.0382	−0.383	–
Chloroform	4.32	0.9774	0.0517	1.205	15.01	1.8548	0.0378	−0.374	–
Ether	4.33	0.9773	0.0517	1.210	14.95	1.8547	0.0377	−0.373	–
CCl_4	4.28	0.9776	0.0518	1.294	14.70	1.8545	0.0374	−0.363	–
MES···Fe^{2+}					*MES···Fe^{2+}*				
Water	5.00	0.9836	0.2219	1.135	7.88	0.9185	0.0211	−0.298	0.087
Ethanol	5.02	0.9835	0.2220	1.155	7.85	0.9183	0.0210	−0.293	0.091
Acetone	5.04	0.9834	0.2231	1.159	7.77	0.9184	0.0209	−0.292	0.091
Chloroform	5.10	0.9835	0.2217	1.262	7.76	0.9178	0.0210	−0.269	0.105
Ether	5.12	0.9834	0.2222	1.269	7.75	0.9177	0.0210	−0.265	0.108
CCl_4	5.14	0.9835	0.2221	1.360	7.55	0.9175	0.0208	−0.245	0.118

of proton donor is the most important. Table 3 shows the stabilization energies, $E^{(2)}$, correspond to charge transfer between oxygen lone pair ($LP_{(O)}$) and $\sigma^*_{(O–H)}$ anti-bond ($LP_{(O)} \rightarrow \sigma^*_{(O–H)}$). As given in this table, the presence of cation–π interaction decreases the $LP_{(O)} \rightarrow \sigma^*_{(O–H)}$ interaction energies and reduces the strength of IMHB. Our results reveal that the highest/lowest $E^{(2)}$ values belong to MES complex in the water/CCl_4 solvents, which is in agreement with their E_{HBs} and have a good relatively linear relationship with the binding energies (see Fig. 6).

Table 3 also displays the charge transfer values ($\Delta q_{(CT2)}$) of corresponding to the HB. For the studied complex in the presence of different solvents, the value of $\Delta q_{(CT2)}$ is determined as the difference between the atomic charge of the oxygen involved in HB of MES···Fe^{2+} complex and the charge of oxygen atom in its corresponding monomer with an equation as: $\Delta q_{(CT2)} = q_O$ (complex)-q_O (monomer). As shown in this table, the least negative charge of the q_O belongs to the MES···Fe^{2+} complex and the most of that corresponds to its similar monomer. It is also apparent from Table 3 that the presence of cation–π interaction enhances the value of $\Delta q_{(CT2)}$ in the non-polar solvents and reduces it in the polar solvents.

3.6 Electronic descriptors

To better understand the nature of the interaction between MES monomer and Fe^{2+} cation, we examine the electronic properties of its corresponding complex in the different media. Higher value of the HOMO of a molecule has a tendency to donate electrons to appropriate acceptor molecule with low energy and empty molecular orbitals. The analysis of the wave function shows the electron excitation correlation with the transition from the ground state to the first excited state. This can be described by an electron excitation from HOMO to LUMO. The energy gap (E_g) is indicated by energy difference between HOMO and LUMO. The E_g is one of the most important factors in determining the stability and reactivity of the molecules [63]. Figure 7 displays the plots of HOMO and LUMO for the MES and BEN complexes in the water solvent.

The quantum molecular descriptors such as softness (S), chemical hardness (η), electronic chemical potential (μ), electronegativity (χ) and electrophilicity index (ω) are listed in Table 4. The hard molecules have a large E_g and soft ones have a small E_g. On the other hand, the high stability is associated with low chemical reactivity of molecules and vice versa [64–66]. Our findings indicate that the maximum and minimum values of E_g and η belong to complexes in the water and CCl_4 solvents, respectively. Hence, the studied complexes in the water solvent are kinetically more stable and those in the CCl_4 solvent show the higher reactivity.

Because these complexes have the values of negative μ, thus they are stable (see Table 4). It is clear that the values of μ enhance in polar solvents and reduce in non-polar solvents. The χ is known as the negative of μ, as: $\chi = -\mu$. As shown in Table 4, the studied complexes in the non-polar solvents have higher electronegativity with respect to the polar ones, which means that they are better electron acceptors. It can also be stated that the least energy gap is associated with the most energy lowering due to electron flow between HOMO and LUMO and vice versa. The results display that the maximum and minimum electrophilicity index belongs to the complexes in the CCl_4 and water solvents, respectively.

From the obtained descriptors in Table 4, it can be concluded that the presence of HB is accompanied with an increment in the S and μ values and reduction in the E_g, η, χ and ω values in the MES complex with respect to the BEN one. The decline of the E_g and η parameters in the MES complex can be attributed to the low chemical stability

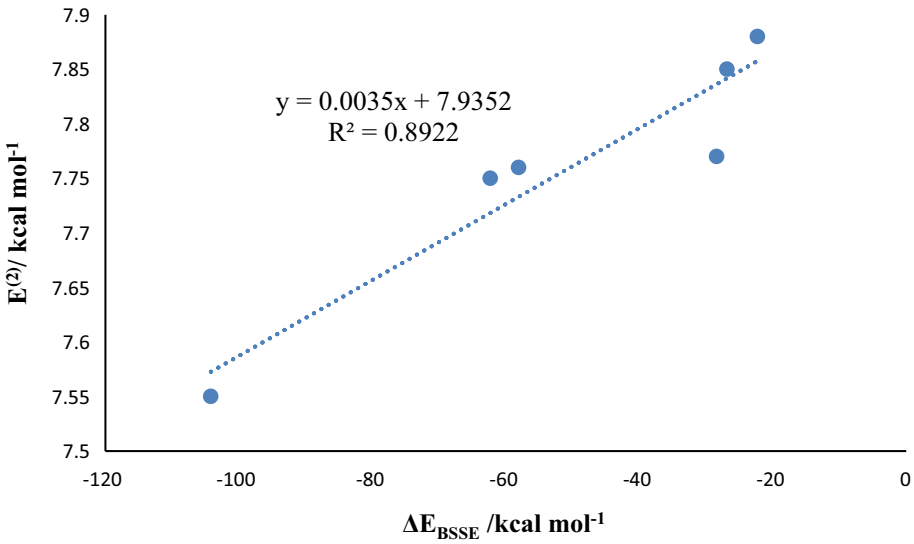

Fig. 6 Correlation between the $E^{(2)}$ and ΔE_{BSSE} values

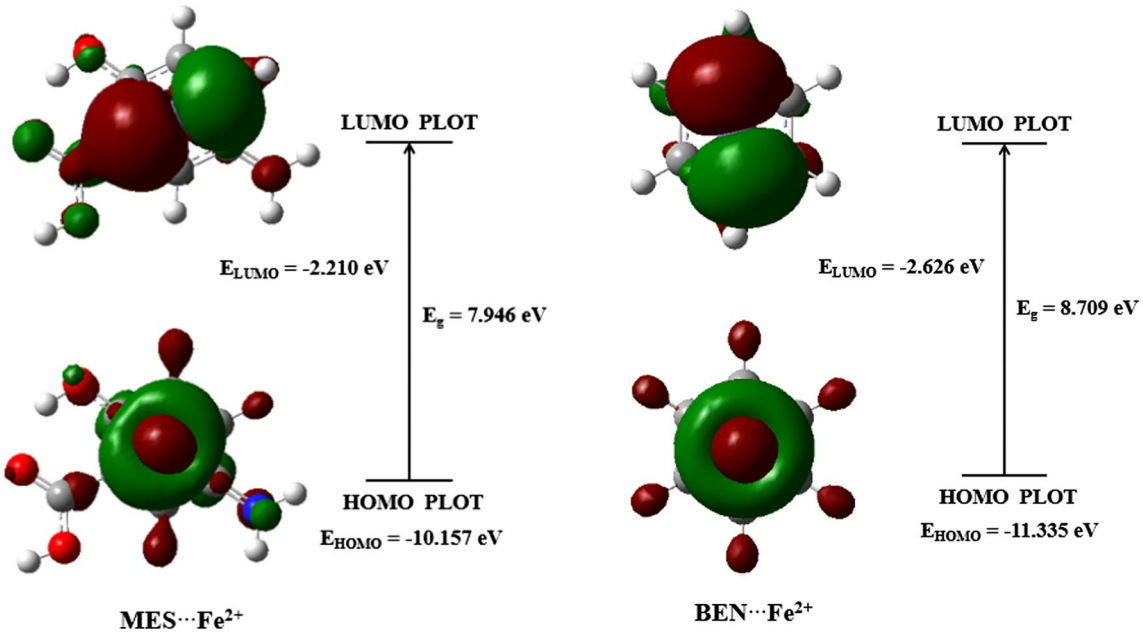

Fig. 7 HOMO and LUMO of MES and BEN complexes in the water solvent as obtained at the wB97XD/6-311++G(d,p) level of theory

Table 4 Values of the HOMO and LUMO energies (E_{HOMO}, E_{LUMO}), energy gap (E_g), chemical hardness (η), softness (S), electronic chemical potential (μ), electronegativity (χ) and electrophilicity index (ω)

	E_{HOMO} (eV)	E_{LUMO} (eV)	E_g (eV)	η (eV)	S (eV^{-1})	μ (eV)	χ (eV)	ω (eV)
MES								
Water	−7.690	−0.007	7.684	3.842	0.130	−3.848	3.848	1.927
Ethanol	−7.683	−0.001	7.682	3.841	0.130	−3.842	3.842	1.921
Acetone	−7.680	0.001	7.681	3.840	0.130	−3.839	3.839	1.919
Chloroform	−7.648	0.027	7.676	3.838	0.130	−3.810	3.810	1.892
Ether	−7.645	0.031	7.676	3.838	0.130	−3.807	3.807	1.888
CCl_4	−7.621	0.053	7.674	3.837	0.130	−3.784	3.784	1.866
BEN···Fe^{2+}								
Water	−11.335	−2.626	8.709	4.355	0.115	−6.981	6.981	5.595
Ethanol	−11.641	−2.941	8.700	4.350	0.115	−7.291	7.291	6.110
Acetone	−11.716	−3.022	8.693	4.347	0.115	−7.369	7.369	6.247
Chloroform	−13.379	−4.742	8.637	4.318	0.116	−9.061	9.061	9.505
Ether	−13.597	−4.969	8.628	4.314	0.116	−9.283	9.283	9.987
CCl_4	−15.670	−7.107	8.563	4.282	0.117	−11.388	11.388	15.145
MES···Fe^{2+}								
Water	−10.157	−2.210	7.946	3.973	0.126	−6.184	6.184	4.812
Ethanol	−10.399	−2.478	7.921	3.961	0.126	−6.439	6.439	5.233
Acetone	−10.480	−2.554	7.926	3.963	0.126	−6.517	6.517	5.359
Chloroform	−11.851	−4.097	7.755	3.877	0.129	−7.974	7.974	8.199
Ether	−12.044	−4.295	7.749	3.874	0.129	−8.170	8.170	8.613
CCl_4	−13.799	−6.171	7.628	3.814	0.131	−9.985	9.985	13.070

and high chemical reactivity of this complex with respect to BEN complex. On the other hand, with the exception of MES complex in the CCl_4 solvent, it can be seen that the coupling of cation–π and IMHB interactions leads to an increase in the E_g, η, χ and ω and a decrease in the S and μ with respect to the parent molecule. As can be observed, there is a different trend for these indices in the presence of cation–π interactions, indicating that these interactions have different effects on each other.

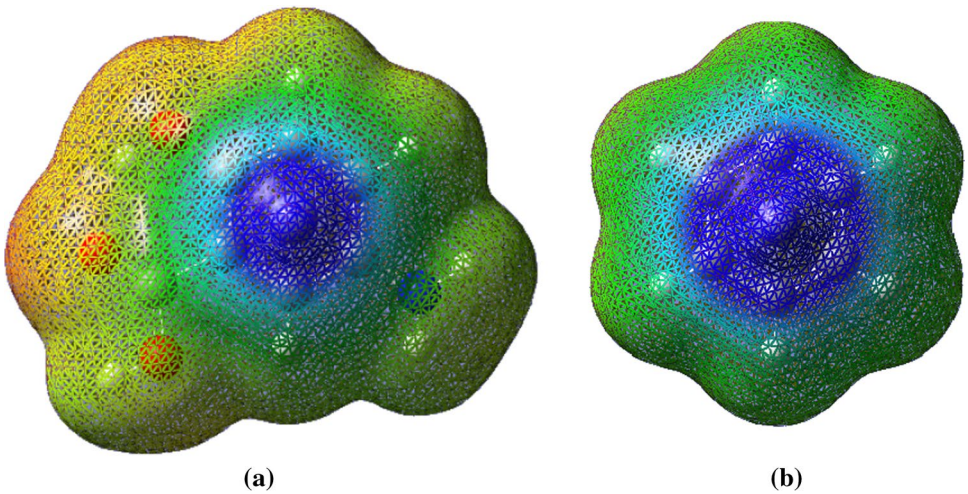

Fig. 8 Electron density isosurface for **a** MES···Fe^{2+} and **b** BEN···$Fe.^{2+}$ complexes calculated by wB97XD method and 6-311++G(d,p) basis set

Among reactivity descriptors, the molecular electrostatic potential (MEP) [67] is a real physical property, which plays an important role in the theoretical chemistry and is widely used in the different areas of science. The MEP 3D plots of MES and BEN complexes calculated by wB97XD method and 6-311++G(d,p) basis set are drawn in Fig. 8. As given in this figure, the electronegative oxygen atoms have the negative potential (indicated by red and yellow colors), and the positive potential site is around the Fe^{2+} cation and the plane of the aromatic ring (indicated by deepest blue color).

4 Conclusions

The DFT calculations are performed to explore the mutual effects between the cation–π and IMHB interactions on the MES···Fe^{2+} complex in the different solvents. The MES molecule and the BEN···Fe^{2+} complex are selected as the set of reference points. These interactions are analyzed by the energetic, geometrical, spectroscopic, topological and charge transfer parameters. The results exhibit that the coexistence of IMHB and cation–π interactions decreases the IMHB strength and increases the cation–π interactions. However, the type of the solvent is key factor that influence the NCIs of the MES complex. The AIM and NBO analyses also confirm these outcomes. The results of electronic descriptors show that there is a different trend in both cation–π and IMHB interactions, which indicates these interactions have different effects on each other. Thus, the interplay between cation–π and IMHB interactions in the analyzed system can be important and might help to understand some biological processes.

Supplementary Information The online version contains supplementary material available at https://doi.org/10.1007/s00214-022-02896-4.

Acknowledgements The support of this work by Vali-e-Asr University of Rafsanjan is acknowledged.

Declarations

Conflict of interest The authors declare that they have no conflict of interest.

References

1. Iacucci M, de Silva S, Ghosh S (2010) Mesalazine in inflammatory bowel disease: a trendy topic once again? Can J Gastroenterol 24:127–133
2. Azad Khan AK, Piris J, Truelove SC (1977) An experiment to determine the active therapeutic moiety of sulphasalazine. Lancet 2:892–895
3. Rubin G, Hungin APS, Chinn D, Dwarakanath AD, Green L, Bates J (2002) Long-term aminosalicylate therapy is under-used in patients with ulcerative colitis: a cross-sectional survey. Aliment Pharmacol Ther 16:1889–1893
4. Oshovsky GV, Reinhoudt DN, Verboom W (2007) Supramolecular chemistry in water. Angew Chem Int Ed 46:2366–2393
5. Saalfrank RW, Maid H, Scheurer A (2008) Supramolecular coordination chemistry: the synergistic effect of serendipity and rational design. Angew Chem Int Ed 47:8794–8824
6. Tian X, Yang R, Chen T, Cao Y, Deng H, Zhang M, Jiang X (2022) Removal of both anionic and cationic dyes from wastewater using pH-responsive adsorbents of L-lysine molecular-grafted cellulose porous foams. J Hazard Mater 426:128121
7. Obireddy SR, Lai W (2021) Preparation and characterization of 2-hydroxyethyl starch microparticles for co-delivery of multiple bioactive agents. Drug Deliv 28(1):1562–1568
8. Feng Z, Li G, Wang X, Gómez-García CJ, Xin J, Ma H, Pang H, Gao K (2022) FeS2/MoS2@RGO hybrid materials derived from polyoxomolybdate-based metal–organic frameworks as high-performance electrocatalyst for ammonia synthesis under ambient conditions. Chem Eng J 445(1):136797
9. Yang W, Liu W, Li X, Yan J, He W (2022) Turning chiral peptides into a racemic supraparticle to induce the self-degradation of MDM2. J Adv Res. https://doi.org/10.1016/j.jare.2022.05.009

10. Hu X, Zhang P, Wang D, Jiang J, Chen X, Liu Y, Zhang Z, Zhong Tang B, Li P (2021) AIEgens enabled ultrasensitive point-of-care test for multiple targets of food safety: aflatoxin B 1 and cyclopiazonic acid as an example. Biosens Bioelectron 182:113188
11. Jeffry GA, Saenger W (1991) Hydrogen bonding in biological structures. Springer-Verlag, Berlin
12. Scheiner S (1997) Hydrogen bonding. Oxford University Press, New York
13. Desiraju GR, Steiner T (1999) The weak hydrogen bond in structural chemistry and biology. Oxford University Press, New York
14. Obireddy SR, Lai W (2021) Multi-component hydrogel beads incorporated with reduced graphene oxide for pH-responsive and controlled co-delivery of multiple agents. Pharmaceutics 13(3):313
15. Yu F, Zhu Z, Li C, Li W, Liang R, Yu S, Xu Z, Song F, Ren Q, Zhang Z (2022) A redox-active perylene-anthraquinone donor-acceptor conjugated microporous polymer with an unusual electron delocalization channel for photocatalytic reduction of uranium (VI) in strongly acidic solution. Appl Catal B: Environ 314:121467
16. Zhou B, Liu Z, Li C, Liu M, Jiang L, Zhou Y, Zhou FL, Chen S, Jerrams S, Yu J (2021) A highly stretchable and sensitive strain sensor based on dopamine modified electrospun SEBS fibers and MWCNTs with carboxylation. Adv Electron Mater 7(8):2100233
17. Zhang Z, Yang Q, Yu Z, Wang H, Zhang T (2022) Influence of Y_2O_3 addition on the microstructure of TiC reinforced Ti-based composite coating prepared by laser cladding. Mater Charact 189:111962
18. Tang X, Wu J, Wu W, Zhang Z, Zhang W, Zhang Q, Zhang W, Chen X, Li P (2020) Competitive-type pressure-dependent immunosensor for highly sensitive detection of diacetoxyscirpenol in wheat via monoclonal antibody. Anal Chem (Washington) 92(5):3563–3571
19. Hong BH, Bae SC, Lee CW, Jeong S, Kim KS (2001) Ultrathin single-crystalline silver nanowire arrays formed in an ambient solution phase. Science 294:348–351
20. Dougherty DA (2007) Cation-π interactions involving aromatic amino acids. J Nutr 137:1504S-1508S
21. Torrice MM, Bower KS, Lester HA, Dougherty DA (2009) Probing the role of the cation–π interaction in the binding sites of GPCRs using unnatural amino acids. Proc Natl Acad Sci USA 106:11919–11924
22. Lhotak P, Shinkai S (1997) Cation–π interactions in calix[n]arene and related systems. J Phys Org Chem 10:273–285
23. Kool ET, Waters ML (2007) The model student: what chemical model systems can teach us about biology. Nat Chem Biol 3:70–73
24. Reddy AS, Sastry GN (2005) Cation [M = H^+, Li^+, Na^+, K^+, Ca^{2+}, Mg^{2+}, NH_4^+, and NMe_4^+] interactions with the aromatic motifs of naturally occurring amino acids: a theoretical study. J Phys Chem A 109:8893–8903
25. Gokel GW, De Wall SL, Meadows ES (2000) Experimental evidence for alkali metal cation−π interactions. Eur J Org Chem 2000:2967–2978
26. Gokel GW, Barbour LJ, De Wall SL, Meadows ES (2001) Macrocyclic polyethers as probes to assess and understand alkali metal cation–π interactions. Coord Chem Rev 222:127–154
27. Tsuzuki S, Yoshida M, Uchimaru T, Mikami M (2001) The origin of the cation/π interaction: the significant importance of the induction in Li^+ and Na^+ complexes. J Phys Chem 105:769–773
28. Rooman M, Liévin J, Buisine E, Wintjens R (2002) cation–π/H-bond stair motifs at protein-DNA interfaces. J Mol Biol 319:67–76
29. Zhang L, Xu Y, Liu H, Li Y, You S, Zhao J, Zhang J (2021) Effects of coexisting Na^+, Mg^{2+} and Fe^{3+} on nitrogen and phosphorus removal and sludge properties using A_2O process. J Water Process Eng 44:102368
30. Li Q, Li W, Cheng J, Gong B, Sun J (2008) Effect of methyl group on the cooperativity between cation-π interaction and NH...O hydrogen bonding. J Mol Struct Theochem 867:107–110
31. Mohammadi M, Khanmohammadi A (2020) Theoretical investigation on the non-covalent interactions of acetaminophen complex in different solvents: study of the enhancing effect of the cation–π interaction on the intramolecular hydrogen bond. Theor Chem Acc 139:141
32. Nowroozi A, Ebrahimi A, Rezvani Rad O (2018) Mutual effects of the cation-π, anion-π and intramolecular hydrogen bond in the various complexes of 1,3,5-triamino-2,4,6-trinitrobenzene with some cations (Li^+, Na^+, K^+, Mg^{2+}, Ca^{2+}) and anions (F^-, Cl^-, Br^-). Struct Chem 29:129–137
33. Alirezapour F, Khanmohammadi A (2020) Computational study of noncovalent interactions within the various complexes of para aminosalicylic acid and Cr^{2+}, Mn^+, Fe^{2+}, Co^+, Ni^{2+}, Cu^+, Zn^{2+} cations: exploration of the enhancing effect of the cation–π interaction on the intramolecular hydrogen bond. Theor Chem Acc 139:180
34. Estarellas C, Escudero D, Frontera A, Quiñonero D, Deyá PM (2009) Theoretical ab initio study of the interplay between hydrogen bonding, cation–π and π–π interactions. Theor Chem Acc 122:325–332
35. Lanier MC, Feher M, Ashweek NJ, Loweth CJ, Rueter JK, Slee DH, Williams JP, Zhu YF, Sullivan SK, Brown MS (2007) Selection, synthesis, and structure–activity relationship of tetrahydropyrido[4,3-d]pyrimidine-2,4-diones as human GnRH receptor antagonists. Bioorg Med Chem 15:5590–5603
36. Rodgers MT, Armentrout PB (2004) A thermodynamic, "vocabulary" for metal ion interactions in biological systems. Acc Chem Res 37:989–998
37. Frisch MJ, Trucks GW, Schlegel HB, Scuseria GE, Robb MA, Cheeseman JR, Montgomery JA Jr, Vreven T, Kudin KN, Burant JC, Millam JM, Iyengar SS, Tomasi J, Barone V, Mennucci B, Cossi M, Scalmani G, Rega N, Petersson GA, Nakatsuji H, Hada M, Ehara M, Toyota K, Fukuda R, Hasegawa J, Ishida M, Nakajima T, Honda Y, Kitao O, Nakai H, Klene M, Li X, Knox JE, Hratchian HP, Cross JB, Bakken V, Adamo C, Jaramillo J, Gomperts R, Stratmann RE, Yazyev O, Austin AJ, Cammi R, Pomelli C, Ochterski JW, Ayala PY, Morokuma K, Voth GA, Salvador P, Dannenberg JJ, Zakrzewski VG, Dapprich S, Daniels AD, Strain MC, Farkas O, Malick DK, Rabuck AD, Raghavachari K, Foresman JB, Ortiz JV, Cui Q, Baboul AG, Clifford S, Cioslowski J, Stefanov BB, Liu G, Liashenko A, Piskorz P, Komaromi I, Martin RL, Fox DJ, Keith T, Al-Laham MA, Peng CY, Nanayakkara A, Challacombe M, Gill PMW, Johnson B, Chen W, Wong MW, Gonzalez C, Pople JA (2003) Gaussian 03 (Revision A.7). Gaussian Inc., Pittsburgh
38. Zhao Y, Truhlar DG (2008) The M06 suite of density functionals for main group thermochemistry, thermochemical kinetics, noncovalent interactions, excited states, and transition elements. Theor Chem Acc 120:215–241
39. Zhao Y, Schultz NE, Truhlar DG (2005) Exchange-correlation functional with broad accuracy for metallic and nonmetallic compounds, kinetics, and noncovalent interactions. J Chem Phys 123:161103-1-161103–4
40. Zhao Y, Schultz NE, Truhlar DG (2006) Design of density functionals by combining the method of constraint satisfaction with parametrization for thermochemistry, thermochemical kinetics, and noncovalent interactions. J Chem Theory Comput 2:364–382
41. Zhao Y, Truhlar DG (2006) A new local density functional for main-group thermochemistry, transition metal bonding, thermochemical kinetics, and noncovalent interactions. J Chem Phys 125:194101-1-194101–18

42. Zhao Y, Truhlar DG (2007) Density functionals for noncovalent interaction energies of biological importance. J Chem Theory Comput 3:289–300
43. Miertus S, Scrocco E, Tomasi J (1981) Electrostatic interaction of a solute with a continuum: a direct utilizaion of AB initio molecular potentials for the prevision of solvent effects. Chem Phys 55:117–129
44. Boys SF, Bernardi F (1970) The calculation of small molecular interactions by the differences of separate total energies. Some procedures with reduced errors. Mol Phys 19:553–566
45. Bader RFW (1990) Atoms in molecules: a quantum theory. Oxford University Press, Oxford
46. BieglerKönig F, Schönbohm J (2002) Update of the AIM2000-program for atoms in molecules. J Comput Chem 23:1489–1494
47. Reed AE, Curtiss LA, Weinhold F (1988) Intermolecular interactions from a natural bond orbital, donor-acceptor viewpoint. Chem Rev 88:899–926
48. Pearson RG (1997) Chemical hardness-applications from molecules to solids. VCH-Wiley, Weinheim
49. Chattaraj PK, Poddar A (1999) Molecular reactivity in the ground and excited electronic states through density-dependent local and global reactivity parameters. J Phys Chem A 103:8691–8699
50. Parr RG, Lv S, Liu S (1999) Electrophilicity index. J Am Chem Soc 121:1922–1924
51. Sen KD, Jorgensen CK (1987) Electronegativity, structure and bonding. Springer Verlag, New York
52. Espinosa E, Molins E (2000) Retrieving interaction potentials from the topology of the electron density distribution: the case of hydrogen bonds. J Chem Phys 113:5686–5694
53. Espionsa E, Souhassou M, Lachekar H, Lecomte C (1999) Topological analysis of the electron density in hydrogen bonds. Acta Crystallogr B 55:563–572
54. Abramov YA (1997) On the possibility of kinetic energy density evaluation from the experimental electron-density distribution. Acta Crystallogr A 53:264–272
55. Grabowski SJ, Sokalski WA, Dyguda E, Leszczyński J (2006) Quantitative classifcation of covalent and noncovalent H-bonds. J Phys Chem B 110:6444–6446
56. Chandra AK, Zeegers-Huyskens T (2004) Theoretical study of $(XYO\cdots H\cdots OXY)^+$ (X, Y=H, F, Cl) systems. From the asymmetrical to the symmetrical $(O\cdots H\cdots O)^+$ hydrogen bonds. J Mol Struct (Theochem) 706:75–83
57. Grabowski SJ, Leszczynski J (2009) The enhancement of X-H$\cdots\pi$ hydrogen bond by cooperativity effects—Ab initio and QTAIM calculations. Chem Phys 355:169–176
58. Bader RFW (1991) A quantum theory of molecular structure and its applications. Chem Rev 91:893–928
59. Garau C, Frontera A, Quiñonero D, Ballester P, Costa A, Deyà PM (2004) Cation–π versus anion–π interactions: energetic, charge transfer, and aromatic aspects. J Phys Chem A 108:9423–9427
60. Parra RD, Ohlssen J (2008) Cooperativity in intramolecular bifurcated hydrogen bonds: an Ab initio study. J Phys Chem A 112:3492–3498
61. Ziółkowski M, Grabowski SJ, Leszczynski J (2006) Cooperativity in hydrogen-bonded interactions: ab initio and "atoms in molecules" analyses. J Phys Chem A 110:6514–6652
62. Balachandran V, Santhi G, Karpagam V, Lakshmi A (2013) Molecular structure, spectroscopic (FT-IR, FT-Raman), NBO and HOMO–LUMO analyses, computation of thermodynamic functions for various temperatures of 2, 6-dichloro-3-nitrobenzoic acid. Spectrochim Acta Part A Mol Biomol Spectrosc 110:130–140
63. Fukui K (1982) Role of frontier orbitals in chemical reactions. Science 218:747–754
64. Pearson RG (1989) Absolute electronegativity and hardness: applications to organic chemistry. J Org Chem 54:1423–1430
65. Zhou Z, Parr RG (1990) Activation hardness: new index for describing the orientation of electrophilic aromatic substitution. J Am Chem Soc 112:5720–5724
66. Faust WL (1989) Explosive molecular ionic crystals. Science 245:37–42
67. Politzer P, Truhlar DG (1981) Chemical applications of atomic and molecular electrostatic potentials. Plenum Press, New York